# Pulsed Device Measurements and Applications

Jonathan Scott, James Grantley Rathmell, *Member, IEEE*, Anthony Parker, *Senior Member, IEEE*, and Mohamed Sayed

***Abstract*— A pulsed measurement system can provide more than just isothermal characteristic data. An off-the-shelf system can determine rapidly the timing necessary for both pulsed-$I$–$V$ and pulsed-$S$-parameter measurements to be isothermal and isodynamic. Instantaneous channel temperature may be determined. Thermal and charge-trapping effects can be separated and time constants measured. Full gain-derivative surfaces can be obtained far more efficiently than by spectral sweep measurements. Characteristics and transient effects following excursions beyond the safe-operating-area and into breakdown may be observed nondestructively.**

## I. Introduction

PULSES were used to obtain GaAs device characteristics free of dispersion effects (chiefly thermal "droop") a decade ago [1]. Once recognized, this gave rise to numerous pulsed-$I$–$V$ (PIV) systems and some reports of their use [2]–[15]. Recently, some of us reported a method by which the timing (or the required duty cycle for the preferred pulse duration) could be found, such that measurements could be relied upon to represent operation unaffected by device thermal and charge-trap time constants [14]. The problem with the method in [14] is that it involves finding a three-dimensional (3-D) surface, only a small part of which—one corner—is important. Furthermore, the literature does not contain many applications of isothermal (constant temperature) and isodynamic (constant charge) measurement.

We present and verify a method for determining timing that does not require the massive amount of data as used in [14], and is thus applicable in the case of measuring $S$-parameters. In addition, we demonstrate that time constants may be found by alternate means, that PIV measurement can be used in place of laborious spectral analysis for characterizing the linearity of devices after the fashion of [16], and because of measurement speed, for observation of transient effects following excursions into breakdown regions. The versatility of pulsed measurement thus assures it a place in the toolbox of GaAs circuit designers.

## II. Measurement System

The measurement system is assembled from commercial instruments and VXI modules and is interconnected as shown in Fig. 1. This system is a refinement of that described in [17],

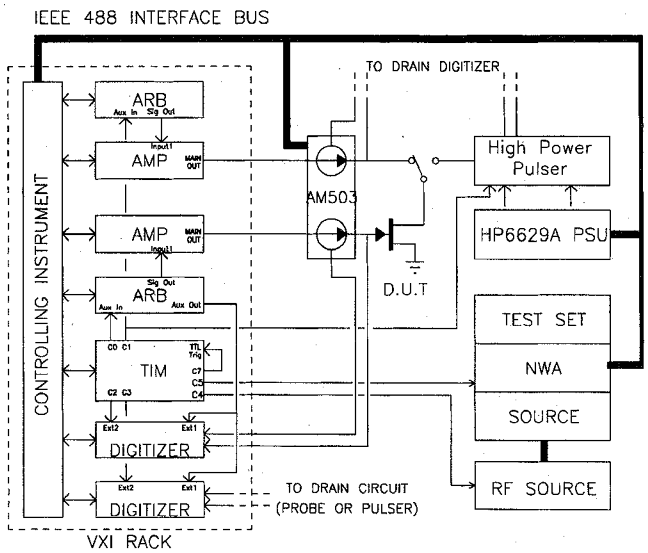


Fig. 1. Block diagram showing interconnection of the various instruments in the measurement system. ARB is an abbreviation of arbitrary function generator, TIM for timing module, PSU for power supply, and NWA for network analyzer.

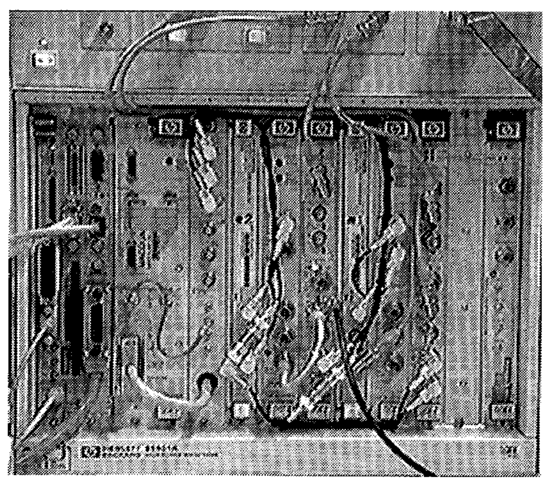

Fig. 2. Photograph of the basic VXI rack, showing also the optional high-power pulser and ribbon cable.

with more sophisticated software and the addition of higher power capability after [11]. A photograph of the VXI rack appears as Fig. 2. The bottom of the high power pulser is visible, showing the high-current ribbon cable [11].

The system offers pulse durations from 100 ns to 25 s with spacing from 100 ns upwards, 12.5 ns event resolution, 12-bit accuracy even at full speed, >10 A current capability,

Manuscript received April 1, 1996
J. Scott and J. Rathmell are with the Department of Electrical Engineering, at the University of Sydney, Sydney 2006, Australia.
A. Parker is with the Department of Electronics, Macquarie University, Sydney 2113, Australia.
M. Sayed is with Hewlett-Packard Systems Division, Santa Rosa, CA 95403 USA.
Publisher Item Identifier S 0018-9480(96)08574-2.

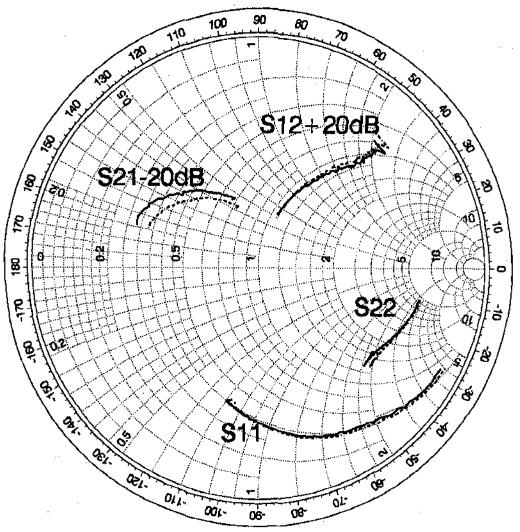


Fig. 3. $S$-parameters for a GaAs FET from 2–10 GHz with pulse measurement times of 2 $\mu$s (solid lines) and 10 ms (dotted lines). The quiescent interval was 10 ms in both cases. Note that $S_{21}$ has been scaled down by 20 dB, and $S_{12}$ up by 20 dB, for plotting clarity.

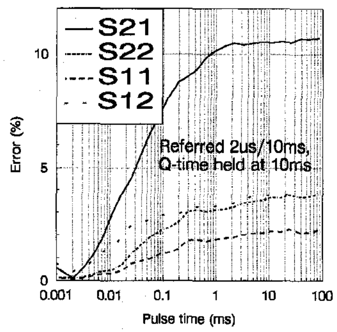


Fig. 4. Average discrepancy from 2–10 GHz between $S$-Parameters of the GaAs FET measured in 2-$\mu$s pulses spaced 10 ms and the $S$-parameters measured with a range of pulse intervals but the same quiescent interval of 10 ms.

pulsed-$I$–$V$ and pulsed $S$-parameter data, scrambled-order measurements, user-specified pulse voltage trajectories, real-time averaging and data reduction, pulse-profiling, and with system software and hardware overheads of typically only a couple of seconds. It is capable of a complete $I$–$V$ characterization of small devices in a few seconds—dramatically shorter than comparable systems, and ideally suited to both production and development environments.

## III. Pulsed $S$-Parameter Timing

Consider the $S$-parameters of the Hewlett-Packard 250-$\mu$m GaAs FET shown in Fig. 3, measured at the point $\{V_{ds} = 6, V_{gs} = 0\}$. One set of $S$-parameters were measured in 2-$\mu$s pulses spaced 10 ms apart, [2 $\mu$, 10 m], with a quiescent point of $\{V_{ds} = 6, V_{gs} = -2\}$, while the others were measured with the FET biased at $\{V_{ds} = 6, V_{gs} = 0\}$. The change in the $S$-parameters, particularly $S_{21}$, as a result of heating and/or charge displacement, is evident. Low-frequency dispersion is clearly visible when comparing the device's pulsed characteristic data with traditional low-frequency measurements for this device [18].

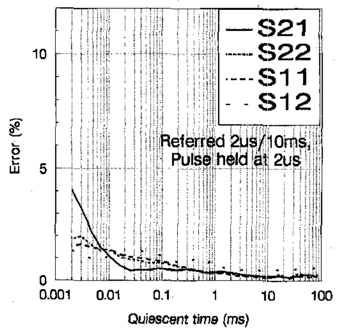


Fig. 5. Average discrepancy from 2–10 GHz between $S$-parameters of the GaAs FET measured in 2-$\mu$s pulses spaced 10 ms and the $S$-parameters measured with a range of quiescent intervals but the same pulse interval of 2 $\mu$s.

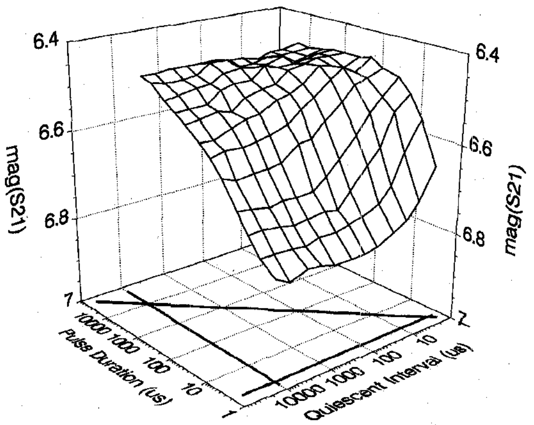


Fig. 6. Magnitude of $S_{21}$ from 2.5–3.5 GHz as a function of pulse and quiescent duration. The 2-D slices are shown projected onto the $xy$-plane below the data surface.

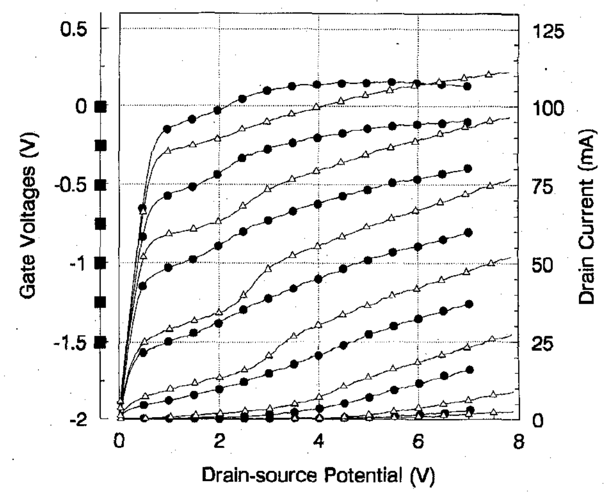


Fig. 7. Drain characteristics of the FET measured at 100 °C with 2-$\mu$s pulses ($\triangle$) and at 20 °C with 10-ms pulses ($\bullet$). The gate-voltage steps corresponding to the characteristic traces are plotted on the left-hand $y$ axis.

What is the significance of this? In a small-signal situation, a device always operates about the operating point. Therefore, $S$-parameters measured at that point, with the device biased at that point, provide all the information a designer requires.

TABLE I
COMPARISON OF S-PARAMETERS AT 3 GHz MEASURED ISOTHERMALLY AT 20°C AND 100°C WITH STEADY-STATE S-PARAMETERS MEASURED AT 20°C. ANGLES ARE IN RADIANS

| S-parameters @3GHz | Isothermal 20C | Isothermal 100C | Steady-state 20C |
|---|---|---|---|
| $S_{11}$ | 0.919∠2.36 | 0.946∠2.36 | 0.937∠2.38 |
| $S_{12}$ | 0.0360∠0.561 | 0.0398∠0.592 | 0.0377∠0.612 |
| $S_{21}$ | 6.15∠-1.08 | 5.46∠-1.05 | 5.45∠-1.04 |
| $S_{22}$ | 0.671∠1.85 | 0.666∠1.83 | 0.681 ∠1.83 |

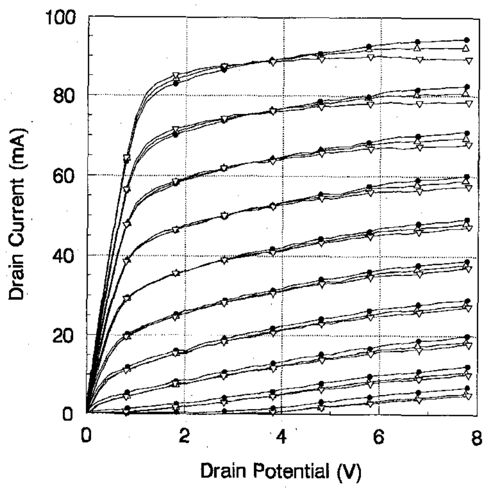


Fig. 8. Characteristic data for an MGF1400 MESFET. One data set is measured in 2-$\mu$s pulses with 1 ms spacing (•), one with 20-$\mu$s pulses (△), and the third with 200-$\mu$s pulses (▽). The quiescent point is maintained at $V_{ds} = 3$ V, $I_{ds} = 42$ mA.

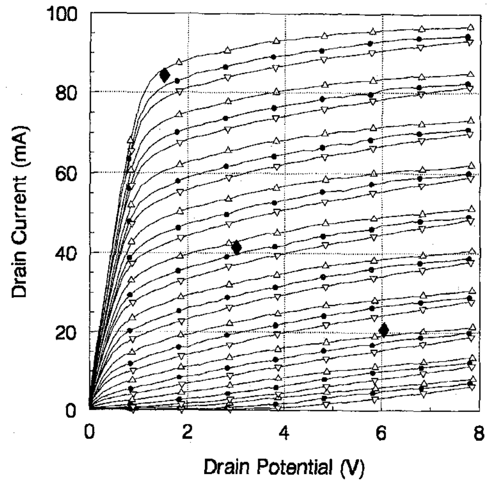


Fig. 9. Characteristic data for an MGF1400 MESFET. All data sets are measured in 2-$\mu$s pulses with 1-ms spacing. The bias points (marked with large diamonds) were at $V_{ds} = 1.5$ V, $I_{ds} = 84$ mA corresponding to data marked (△), $V_{ds} = 3$ V, $I_{ds} = 42$ mA corresponding to data marked (•), and $V_{ds} = 6$ V, $I_{ds} = 21$ mA corresponding to data marked (▽).

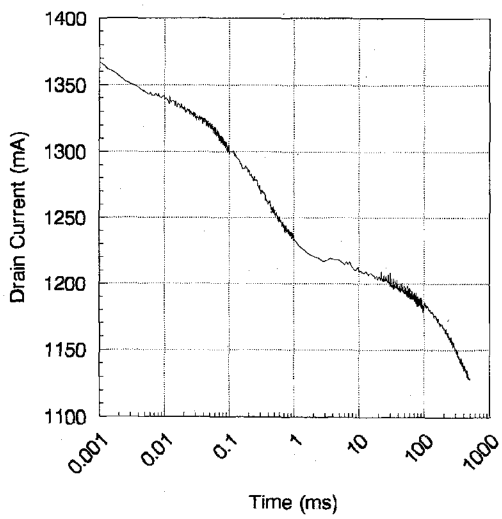


Fig. 10. Drain current of a FET subjected to a pulse to $V_{ds} = 5$ V and $V_{gs} = 0.5$ V, from $V_{ds} = 0$ V, and $V_{gs} = 0.0$ V, plotted as a function of time on a logarithmic scale.

However, in a large-signal situation the device will typically follow some reactive load trajectory. When delivering full power, instantaneous excursions may include extremes of the $V_{ds}/I_{ds}$ plane. In this case, the behavior of the device will be characterized not by the $S$-parameters measured at the nominal operating point, but by the parameters at the extreme, *with the device biased at the nominal operating point as before*. These two cases may be different, even for two points in the normal, forward-active region, as exemplified by the data in Fig. 3. The situation is naturally much worse when excursions include the controlled-resistance or subthreshold regions.

What pulse duration and pulse spacing will ensure isothermal and isodynamic conditions in the channel during measurement? To investigate the effect of this timing the $S$-parameters are measured while varying the pulse duration and holding the quiescent time interval (interpulse spacing) constant at 10 ms. For each measurement, the discrepancy between the parameters so obtained and those found in a "reference" case of $\{6, 0\}/[2\ \mu\ 10\ \mathrm{m}]$ are calculated. The discrepancy or error has been calculated as the average over all frequencies of the complex distance between each $S$-parameter. (We measured at 51 frequencies equispaced between 2–10 GHz.) The result is plotted in Fig. 4. Observe firstly that the traces flatten out above 1 ms, indicating that the values of the parameters have settled to their steady-state values after the transition between quiescent and pulse points. This implies that there is little to be gained in this instance from settling intervals greater than 1 ms. The channel reaches equilibrium after this interval. The traces also flatten out for small intervals. Note that the curves dip to zero error as they pass the reference point $\{6, 0\}/[2\ \mu\ 10\ \mathrm{m}]$. The fact that the traces are only just leveling out at the 1 $\mu$s point suggests that 1 $\mu$s is only barely short enough for isothermal characterization of this device. (Bias networks set a lower limit of $\approx$1 $\mu$s for these tests. The RF equipment lower limit is just under 500 ns, and the PIV limit 100 ns.)

The conclusions in the preceding paragraph rest on the assumption that the inter pulse interval—10 ms—is sufficiently long. Consider now the plot of Fig. 5. Here the pulse time is held short, and the quiescent interval varied. The traces now settle for quiescent times in excess of about 200 $\mu$s, although there is a small change as duty cycle extends from 1% to below 0.1%. This confirms that the choice of 10 ms was sound. The

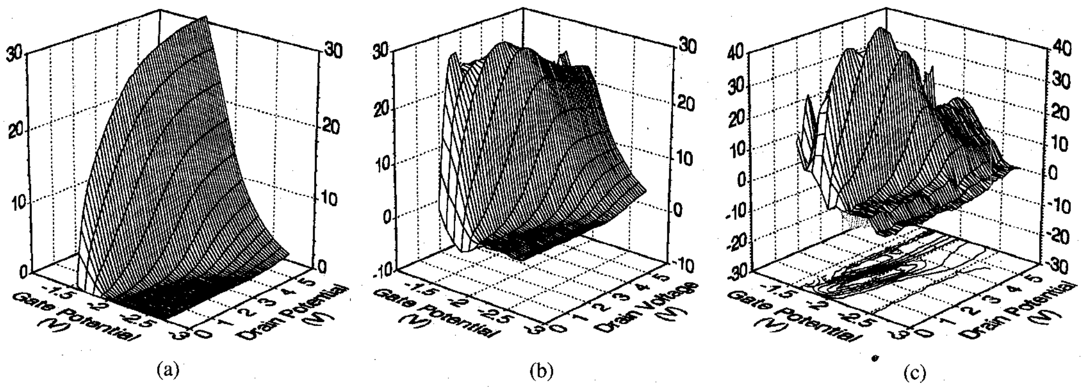


Fig. 11. Plot of $g_m$ (a) and its first (b) and second (c) derivative plotted against gate and drain voltages in the subthreshold region of a MESFET. This is a set of so-called "gain-derivative surfaces." Note the contour plot projected onto the $xy$-plane of the $g_m''$ graph, showing the crest-and-trough shape along a slice of constant drain potential.

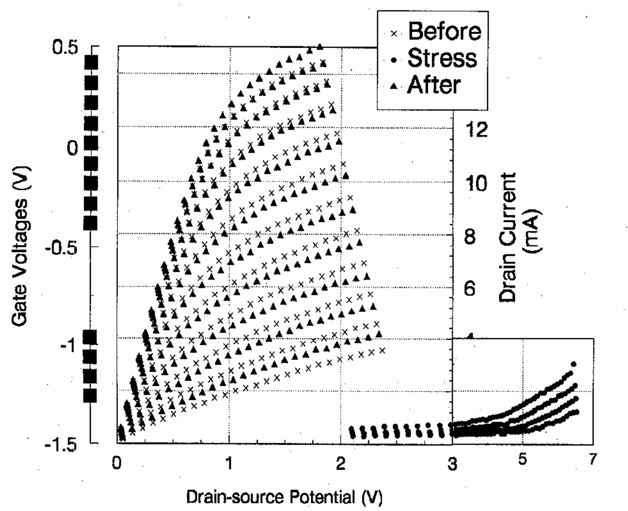


Fig. 12. Pulsed-$I$–$V$ characteristics before and after a series of stress pulses, plotted along with the response to the stressing pulses.

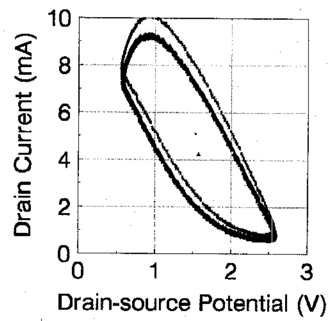


Fig. 13. Drain load trajectories before and after nondestructive pulse stressing of a Monofast FET.

conclusion is that a pulse of duration below 2 $\mu$s with a duty cycle below 1% will yield isothermal, isodynamic $S$-parameter data.

Much of the error surface for the $S$-parameter measurements appears as Fig. 6. As described in [14], the optimum corner suggests the same timing deduced above, confirming the result. It has been shown previously [18] that these limits cannot reliably be found via a single slice through the surface, but the time taken to gather two slices is dramatically less than that required to obtain the surface of Fig. 6, let alone a surface such as that in [14]. The importance of determining this information—the optimum timing for a given device—is appreciated when it is realized that there are situations where a duty cycle of 0.0001%, or 1 million to one, is required [19].

## IV. Channel Temperature Measurement

The temperature reached in the channel of a FET as a result of dissipation during a measurement may be easily determined. Direct heating of the device during isothermal measurement should be able to cause a change in $S$-parameters similar to that occurring between isothermal and steady-state measurement. Table I compares values of $S$-parameters measured isothermally at 20°C and 100°C with steady-state parameters measured at 20°C; the latter resemble the isothermal 100°C set quite closely. The pulsed drain characteristics at 100°C are plotted in Fig. 7, along with the 20°C steady-state characteristics. Note that the dc and 100°C pulsed-$I$–$V$ curves intersect near $\{6, 0\}$. It may be inferred that the observed changes are a result of change in device channel temperature, and hence the channel has reached 100°C when measured at room temperature by conventional, steady-state, $S$-parameter measurement.

## V. Trapping Effects

Figs. 8 and 9 show how charge trapping effects may be identified as distinct from thermal effects. In Fig. 8, three sets of drain characteristics are presented. Each set has drain current values measured after a different pulse interval; the longer the pulse, the more time the channel has to approach its equilibrium point. The longer the pulse, the more the channel heats during measurement and the more the characteristic droops, as expected. However in Fig. 9, the pulse timing remains constant, but the quiescent point is changed. The chosen quiescent operating points give equal power dissipation, and hence identical quiescent temperature. Since the pulses are short, the measurement is isothermal, and the change that is observed must result from changes in trapped charge, brought about by the change in quiescent field. (The $Q$-point trajectory is isothermal but not isodynamic.)

The values of time constants may be determined from the response to a step change in gate and drain potential. Fig. 10 gives an example of another FET where drain current is plotted against log-time to expose time constants. Subsequent processing as outlined in [20] can yield values that may be used in device models. If it is desired to identify only time constants associated with charge effects, the stimulus transition needs simply to be chosen so as to keep dissipation constant as was done for Fig. 9.

## VI. Gain Derivative Extraction

The $g_m$-compression of HEMT's is one example of unusual nonlinear behavior of concern to designers. The first derivatives of drain current ($g_m = \partial I_d/\partial V_{gs}$ and $g_{ds} = \partial I_d/\partial V_{ds}$) are not the only ones of concern: knowledge of the second and third derivatives may be used to good effect in circuits [16] and [24], while the behavior of the third derivative is a powerful method to evaluate the viability of various device models [21] and [22]. Normally, the linearity information is measured by means of small-signal ac sources and a spectrum analyzer. Such information may be extracted using a PIV system directly. Fig. 11 shows the variation of $g_m$ and its two derivatives for an MGF1400 MESFET against gate and drain potential. This is a set of gain-derivative surfaces after [16], but obtained without the use of synthesized sources, spectrum analyzer or special filters. The contour plot below the $g_m''$ surface makes it possible to see the adjacent positive and negative excursions along a slice of constant drain-source potential, as reported in [22, Fig. 3]. A similar third-derivative characteristic may be found from $S$-parameter measurements [23].

## VII. Stress Effects

Considerable attention has been paid recently to permanent and/or long-term effects in III–V FET's related to charge accumulation in various regions of devices, and their substrate and passivation layers [25] and [26]. The system can apply brief, controlled pulses to mimic full-power RF operation or to induce nondestructive breakdown. Fig. 12 displays a set of traces representing a FET being characterized before, during and after stressing by means of high voltage gate-drain pulses.[1]

The measurement system can also impose stimulus signals representative of an RF load-line. Fig. 13 presents "before and after" simulated complex load line trajectories for a Monofast FET. Between the two (identical) load-line style tests, it was exposed to short pulses sufficient to break down the gate-drain junction. The trajectories shown were made by establishing a series of $\{V_{gs}V_{ds}\}$ voltages yielding the pseudo-elliptical voltage-current loops displayed, interspersed with returns to the quiescent point, shown by the single symbol near the center of the loop.

[1] The FET used in this example has been fabricated with an isolated metal island specifically to investigate the effect.

## VIII. Conclusion

Accurate device characterization requires data measured under isothermal and isodynamic conditions. This in turn requires identification of the pulse and inter pulse intervals needed to give results free of device history effects. The ability to apply such fast stimuli to a device also permits measurement of instantaneous channel temperature, thermal and trapping time constants, and derivative characteristics. Complex load and transient stress effects may be imposed and device response measured. Results of these measurements give designers new power and insight.

## Acknowledgment

The authors wish to thank I. Thayne at Glasgow University for the supply of special devices, and Hewlett-Packard's Santa Rosa Systems Division, for loan of equipment.

## References

[1] T. M. Barton, C. M. Snowden, J. R. Richardson, and P. H. Ladbrooke, "Narrow pulse measurement of drain characteristics of GaAs MESFET's," *Electron. Lett.*, vol. 23, pp. 686–687, 1987.

[2] M. Paggi, P. H. Williams, and Jose M. Borrego, "Nonlinear GaAs MESFET modeling using pulsed gate measurements," *IEEE Trans. Microwave Theory Tech.*, vol. 36, no. 36, pp. 1593–1597, Dec. 1988.

[3] A. Platzker, A. Palevski, S. Nash, W. Struble, and Y. Tajima, "Characterization of GaAs devices by a versatile pulsed *I-V* measurement system," in *IEEE MTT-S Dig.*, 1990, pp. 1137–1140.

[4] W. Struble, S. L. G. Chu, M. J. Schindler, Y. Tajima, and J. Huang, "Modeling intermodulation distortion in GaAs MESFET's using pulsed *I-V* characteristics," in *Tech. Dig. IEEE GaAs IC Symp.*, Monterey, CA, Oct. 20–23, 1991, pp. 179–182.

[5] A. Parker and J. Scott, "New method for comprehensive characterization of MES/MOD/MOS FET's," in *Proc. IEEE Int. Symp. Circ. Syst.*, Chicago, IL, May 3–6, 1993, pp. 1093–1096.

[6] T. Fernandez, Y. Newport, J. M. Zamanillo, A. Tazon, and A. Mediavilla, "Modeling of operating point non linear dependence of $I_{ds}$ characteristics from pulsed measurements in MESFET transistors," in *Eur. Microwave Conf.*, Madrid, Spain, 1993, pp. 518–521.

[7] J. P. Teyssier, M. Campoveccio, C. Sommet, J. Portilla, and R. Quéré, "A pulsed $S$-parameters measurement setup for the non-linear characterization of FET's and bipolar power transistors," in *Eur. Microwave Conf.*, Madrid, Spain, 1993, pp. 489–493.

[8] R. Quéré, J. Obregon, and J. P. Teyssier, "Non-linear characterization and modeling of semiconductor devices: An integrated approach," in *Eur. Microwave Conf. Workshop Proc.*, Madrid, Spain, 1993, pp. 18–21.

[9] T. Fernandez, Y. Newport, J. M. Zamanillo, A. Mediavilla, and A. Tazon, "High speed automated pulsed $I/V$ measurement system," in *Eur. Microwave Conf.*, Madrid, Spain, 1993, pp. 494–496.

[10] B. Taylor, M. Sayed, and K. Kerwin, "A pulse bias/RF environment for device characterization," in *IEEE Automated RF Test Group (ARFTG)*, Dec. 2, 1993.

[11] S. Prichett, R. Stewart, J. Mason, G. Brehm, and D. Christie, "Precision pulsed $I$–$V$ system for accurate GaAs device $I$–$V$ plane characterization," in *IEEE MTT-S Int. Microwave Symp. Dig.*, May 23–27, 1994, pp. 1353–1356.

[12] J. Scott, M. Sayed, P. Schmitz, and A. Parker, "Pulsed-bias/Pulsed-RF device measurement system requirements," in *24th Eur. Microwave Conf.*, Cannes, France, Sept. 1994, pp. 951–961.

[13] A. Jastrzebski, "Characterization and modeling of temperature and dispersion effects in power MESFET's," in *Proc. 24th Eur. Microwave Conf.*, Cannes, France, Sept. 5–8, 1994, pp. 1319–1324.

[14] A. Parker and J. Scott, "Method to determine correct timing for pulsed-$I/V$ measurement of GaAs FET's," *Electron. Lett.*, vol. 31, no. 19, pp. 1697–1698, Sept. 14, 1995.
[15] P. H. Ladbrooke, A. K. Jastrzebski, R. J. Donarski, J. P. Bridge, and J. E. Barnaby, "Mechanism of drain current droop in GaAs MESFET's," *Electron. Lett.*, vol. 31, no. 21, pp. 1875–1876, Oct. 12, 1995.
[16] D. R. Webster, J. B. Scott, and D. G. Haigh, "Control of circuit distortion by the derivative superposition method," *Microwave Guided Wave Lett.*, vol. 6, no. 3, Mar. 1996.
[17] J. Scott, A. Parker, and M. Sayed, "RF, pulsed-$I$–$V$, device measurement system in VXI," in *Workshop Appl. Radio Sci.*, Canberra, Australia, June 25–27, 1995.
[18] A. Parker, J. Scott, J. Rathmell, and M. Sayed, "Determining timing for isothermal pulsed-bias $S$-parameter measurements," in *IEEE MTT-S Int. Symp. Dig.*, San Francisco, CA, June 17–24, 1996, pp. 1707–1710.
[19] J. Scott, A. Parker, J. Rathmell, and M. Sayed, "New applications for pulsed/isothermal test system," in *IEEE Automat. RF Test Group Meet.*, San Francisco, CA, June 24, 1996.
[20] D. N. Swingler, "A differential technique for the Fourier transform processing of multicomponent exponential functions," *IEEE Trans. Biomed. Eng.*, vol. BME-24, no. 4, pp. 408–410, July 1977.
[21] A. E. Parker and D. J. Skellern, "Improved MESFET characterization for analog circuit design and analysis," in *1992 Int. GaAs IC Symp. Tech. Dig.*, Miami Beach, FL, Oct. 4–7, 1994, pp. 225–228.
[22] A. E. Parker, "Implementing SPICE models with high-order continuity and rate dependence," *IEE Proc. Circ., Dev. Syst.*, vol. 141, no. 4, pp. 251–257, Aug. 1994.
[23] S. A. Maas and D. Neilson, "Modeling GaAs MESFET's for intermodulation analysis," *Microwave J.*, pp. 295–298, May 1991.
[24] A. Parker and J. Scott, "Intermodulation nulling in GaAs MESFET's," *Electron. Lett.*, vol. 29, no. 22, Oct. 28, 1993.
[25] J. C. M. Hwang, "Gradual degradation under RF overdrive of MESFET's and PHEMT's," in *GaAs IC Symp.*, San Diego, CA, Oct. 1995, pp. 81–84.
[26] G. Meneghesso, E. De Bortoli, P. Cova, and R. Menozzi, "On temperature and hot electron induced degradation in AlGaAs/InGaAs PM-HEMT's," in *IEEE Workshop on High Performance Electron Devices for Microwave and Optoelectronics Applications (EDMO 95)*, London, U.K., Oct. 1995, pp. 98–103.

**Jonathan Scott** was born in Brisbane, Australia, in 1956. He received B.S. and B.E. degrees from the University of Sydney in 1977 and 1979, respectively, the M.S. degree from Sydney University in 1986, and the Ph.D. degree in 1996.

He has worked as a consultant in a variety of industries including radar and analog signal processing. Since 1988, he has been the manager of the Sydney Microwave Design Resource Centre, and is a Senior Lecturer in the Department of Electrical Engineering at the University of Sydney. In 1993, he held a British Telecom Research Fellowship. Since 1994, he has been working with Hewlett-Packard Systems Division in Santa Rosa, and Macquarie University in Sydney on nonlinear measurement and modeling of GaAs FET devices. In 1995, he was a visitor at University College, London, and a guest lecturer at the University of Western Sydney. He is presently a Visiting Fellow at Macquarie University.

Dr. Scott is a member of the Audio Engineering Society (AES), and the Institute of Radio and Electronics Engineers (IREE). He received the Electrical Engineering Foundation medal for Excellence in Teaching in 1994.

**James Grantley Rathmell** (M'89) was born in 1955 in Australia. He received the B.S., B.E., and Ph.D. degrees in 1977, 1979, and 1988, respectively, from the University of Sydney, Australia.

He worked in radio astronomy from 1979–1981, with both the Molonglo and Fleurs aperture synthesis telescopes. With these programs he worked on signal and image analysis, and the design of various microprocessor-based control hardware and software. From 1982–1986, he worked on gate array and VLSI design of digital integrated circuits, principally for communications, and researched the behavioral modeling of digital circuits. During this time, he was a member of the teaching staff at the University of Sydney. He joined The Nucleus Group in 1986, to work on the design of biomedical equipment. He managed the research and development of advanced ultra sound imaging equipment. In 1989, he returned to the University of Sydney, where he is currently a Senior Lecturer in digital systems and engineering management. During this time, he has worked on fiber-optic video-conferencing and digital audio signal processing. In 1995, he joined collaborative work with Macquarie University on the development of pulsed-bias and pulsed $S$-parameter characterization of microwave devices. His main contribution in this has been in signal processing algorithms and measurement control software.

Dr. Rathmell is the chairperson of the Publications Committee of The Institution of Radio and Electronic Engineers, Australia. He is a Senior Member of The Institution of Radio and Electronic Engineers, Australia.

**Anthony Parker** (S'84–M'84–S'86–M'90–SM'95) received the B.S., B.E., and Ph.D. degrees from the University of Sydney in 1983, 1985, and 1992, respectively.

He joined Australia's Overseas Telecommunications Commission in 1993. He managed the VHF Seaphone service upgrade, designed radio and microwave systems, and worked on small, satellite earth-station installations. In 1986, he began work on design techniques and circuit models for gallium arsenide microwave technology. This research began in 1986 at the University of Sydney in collaboration with the Division of Radiophysics of Australia's Commonwealth Scientific and Industrial Research Organization. In 1990, he joined Macquarie University, Sydney, and is now a Senior Lecturer and Curriculum Director of the Bachelor of Technology Degree. As a visiting researcher at University College, London in 1993, he began a continuing project on design of low-distortion communications circuits. He has developed accurate circuit simulation techniques, such as used in the Parker—Skellern FET model now installed in Pspice. While a consultant for the M/A-COM Microwave Semiconductor Division, MA, in the first half of 1994, he worked on MESFET model extraction and circuit simulation techniques.

Dr. Parker has authored or co-authored more than 50 publications. He is a member of the Institution of Radio and Electronic Engineers, Australia, and a member of the Publications Committee of the Institution of Radio and Electronic Engineers Society.

**Mohamed Sayed**, photograph and biography not available at the time of publication.